ICF10063OR

MICROSTRUCTURE-PROPERTY DAMAGE ANALYSIS OF NOTCH TENSILE TESTS

M. F. Horstemeyer[1] , Ken Gall[2], K.W. Dolan[3], A. Waters[3], J.J. Haskins[3], D.E. Perkins[3], A. M. Gokhale[4], and M.D. Dighe[4]

[1]Center for Materials and Engineering Sciences, Solid & Material Mechanics Dept, Sandia National Laboratories, Livermore, CA 94550,
[2]Mechanical Engineering Dept., University of Colorado, Boulder, Co 80309,
[3]Lawrence Livermore National Laboratory, Livermore, CA 94550
[4]Materials Science and Engineering Department, Georgia Institute of Technology, Atlanta, GA 30332

ABSTRACT

Microstructure-property relations related to void nucleation, growth, and coalescence in A356 aluminum notch specimens were determined from a combination of experiments, finite element analysis, nondestructive analysis, and image analysis. Notch Bridgman tension experiments were performed on specimens to failure and then other specimens were tested to 90%, 95%, and 98% of the failure load. The specimens were evaluated with nondestructive x-ray tomography and optical image analysis. Finite element simulations of the notch tests were performed with an elastic-plastic internal state variable material model that incorporated the pertinent microstructures (silicon particle volume fraction and size distribution and porosity volume fraction and size distribution). The various methods all corroborated the same damage progression.

KEYWORDS

notch, finite element analysis, image analysis, x-ray tomography, A356 aluminum, damage, failure, porosity

RESULTS AND DISCUSSION

Computed tomography and optical microscopy results were used with finite element modeling in order to link microstructural features to the mechanical response of a cast A356 aluminum alloy. In particular, we focused on the damage progression by analyzing different notch test specimens which were loaded to different strain levels. Each of these specimens were analyzed nondestructively by computed tomography and

then sectioned for optical microscopy. The data were then compared to finite element simulations. In the finite element simulations, an internal state variable plasticity model was used [1] with rate equations for void nucleation, growth, and coalescence [2]). The rate equations were initialized with the volume fraction of voids, volume fraction of second phase particles, and the size of second phase particles.

Several issues related to size should be raised. The computed tomography results had a minimum resolution of 28 microns, and the optical microscopy had a minimum resolution of 0.5 microns. The average silicon particle size was 4 microns; the average initial pore size was 50 microns; and the average dendrite cell size was 25 microns.

Because variability in porosity levels and silicon particle distributions are evidenced in cast A356 aluminum structural components, we exercised the material model in the finite element analyses with homogeneous and random distributions based on size. Moreover, we included different initial void volume fractions that could arise from different casting processes. The notch test simulation results showed that the initially randomized porosity gives lower failure displacements than the homogeneous case. This difference lessened as the initial porosity level increased. The failure displacements ranged from approximately 0.05 mm to 0.11 mm (the gage radius was 4.7625 mm). The experimental failure displacement was approximately 0.11 mm indicating that our initial porosity assumptions were comparable to the experimental specimens.

The progression of damage in notch tensile specimens for this cast A356 aluminum alloy gives an understanding of the role of the nonhomogeneous distribution of initial porosity and second phase silicon on the final failure state. With this understanding, we now focus on comparisons of the finite element simulations and experimental results, which include image analysis and x-ray tomography of the physical specimens.

At a higher initial porosity level, pore growth and coalescence mechanism is more dominant than the void nucleation from the second phase material, albeit both interact together in the damage process. We summarize different initial porosity levels and distributions in Table 1 with data from the x-ray tomography. The finite element results show that porosity levels comparable to the experimental results can be achieved by the right combination of initial porosity and distribution level. It appears that three of the cases could match the experimental data, but clearly the homogeneous distribution with with an initial porosity of 0.0001 does not correlate well. Because three different specimens were used in the tests and the same simulation was used for the FEM data results, distinguishing whether the initial distributions were homogeneous or random is difficult. Clearly, the trends are similar, which suggests that the damage progression was driven more by the notch geometry and not the initial microstructure in this particular case.

Table 1. Peak void volume fractions within notch specimen at different strain levels.

Failure load %	x-ray tom.	FEM (ϕ_i = 0.0001 homog.)	FEM (ϕ_i = 0.0001 random)	FEM (ϕ_i = 0.001 homog.)	FEM (ϕ_i = 0.001 random)
90	0.028	0.003	0.056	0.069	0.071
95	0.186	0.017	0.124	0.155	0.168
98	0.451	0.123	0.445	0.483	0.520

Finite element and x-ray tomography results were not only determined over the highest spatial resolution, but comparisons to the image analysis results were considered by averaging over a larger region (three different sections). Comparisons were performed on specimens that were 90%, 95%, and 98% of failure.

Figure 2 shows a comparison of the image analysis montage, x-ray tomography picture, and a contour plot of total void volume fraction from the finite element simulation in which an initially random porosity level of 0.001 was assumed for the 98% of fracture load case. Note that small and large region averages are included for comparison. Figure 2a shows the x-ray tomography result; Figure 2b is a high resolution area montage that comprises 100 microstructural fields at 100X magnification of the microstructure and illustrates the porosity distribution in the entire notch region. The differences in the montage and x-ray tomography picture arise because the image analysis only shows one plane cutting axially through the specimen. The x-ray tomography results average 360 planes rotated at one degree throughout the specimen. As one would expect, the x-ray tomography results slightly differ than the image analysis results but closer the finite element analysis, since the same axisymmetric assumptions are included in the simulations. Although the peak values are different between the x-ray tomography and finite element simuations, the maximum void volume fraction is largest at z=0 in the axial direction for both and decreases as the direction z increases or decreases.

Figure 1 is the quantitative data retrieved from Figure 2. When comparing the x-ray tomography and FEM results, one can see that the FEM peak void volume fraction (total damage) is slightly higher (52% to 45%). This may arise due to the initial porosity level assumption. Since we did not quantify the initial porosity states, we would expect some void volume fraction differences. See Table 1 for other initial configurations. Other simulation comparisons at 90% and 95% of failure showed similar qualitative trends as Figures 1 and 2.

Differences in the x-ray tomography and optical image results arose because each of the measurements were from different specimens which had different initial porosity levels, while the finite element simulations were from a single calculation using an initial starting porosity level of 0.001 that provided qualitative damage progression agreement with both the x-ray tomography and optical metallography..

SUMMARY

Microstructure-property relations for damage have been quantified and confirmed by independent methods of evaluation for a cast A356 aluminum alloy notch tensile testing. The methods include experiments; x-ray computed tomography; optical microscopy/stereology metallography image analysis; and finite element simulations that include a history dependent elastic-plastic internal state variable plasticity model involving evolution equations for void nucleation, growth, and coalescence.

ACKNOWLEDGEMENTS

The work by M.F. Horstemeyer and Ken Gall was performed at the U.S. Dep. of Energy Sandia National Laboratories under contract DE-AC04-94AL85000. The work of K.W.

Dolan, J.J. Haskins, and D.E. Perkins was performed under the U.S. Department of Energy Lawrence Livermore National Laboratory under contract W-7405-Eng-48.

REFERENCES

1. Bammann, D.J., Chiesa, M.L., Horstemeyer, M.F. and Weingarten, L.I. (1993) Failure in Ductile Materials Using Finite Element Methods. *Structural Chrashworthness and Failure*, eds. N. Jones and T. Weirzbicki, Elsevier Applied Science.

2. Horstemeyer, M. F., Lathrop, J., Gokhale, A. M., and Dighe, M (2000) Modeling Stress State Dependent Damage Evolution in a Cast Al-Si-Mg Aluminum Alloy, *Theoretical and Applied Mechanics,* **33**, 31-47.

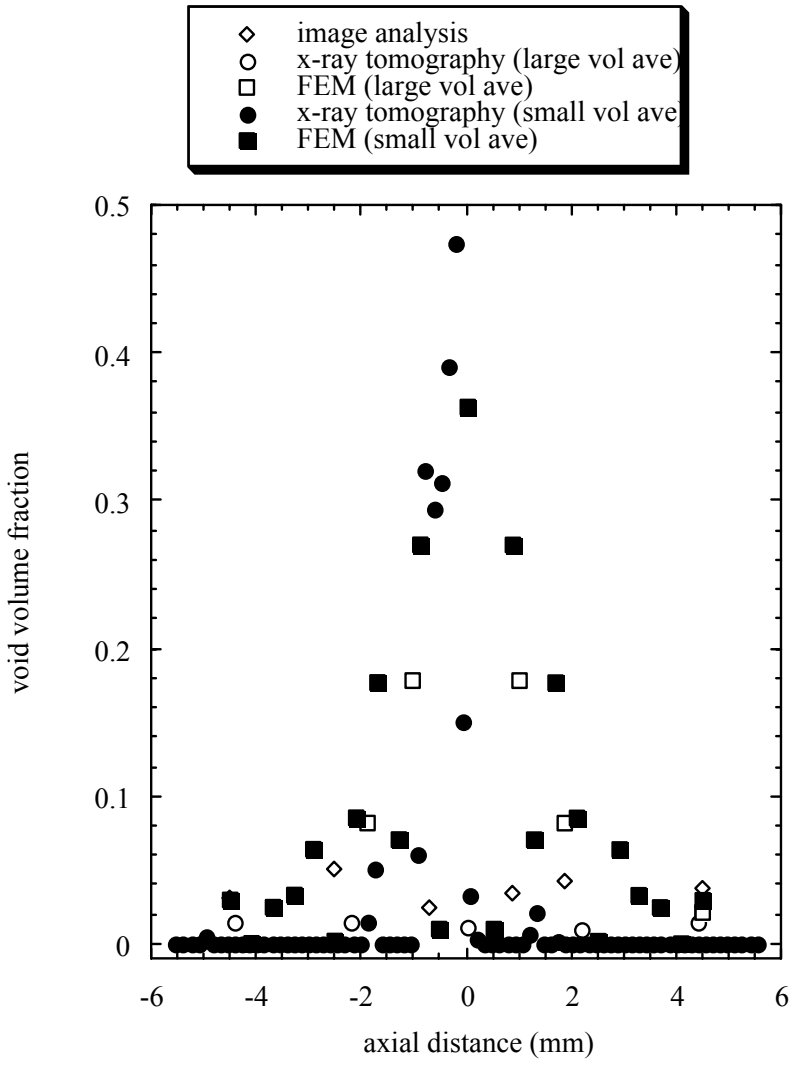

Figure 1. Total void volume fraction along axial distance determined from 98% of failure load specimen from x-ray tomography, image analysis, and finite element analysis with averaged regions similar to those taken for the tomography and image analysis measurements.

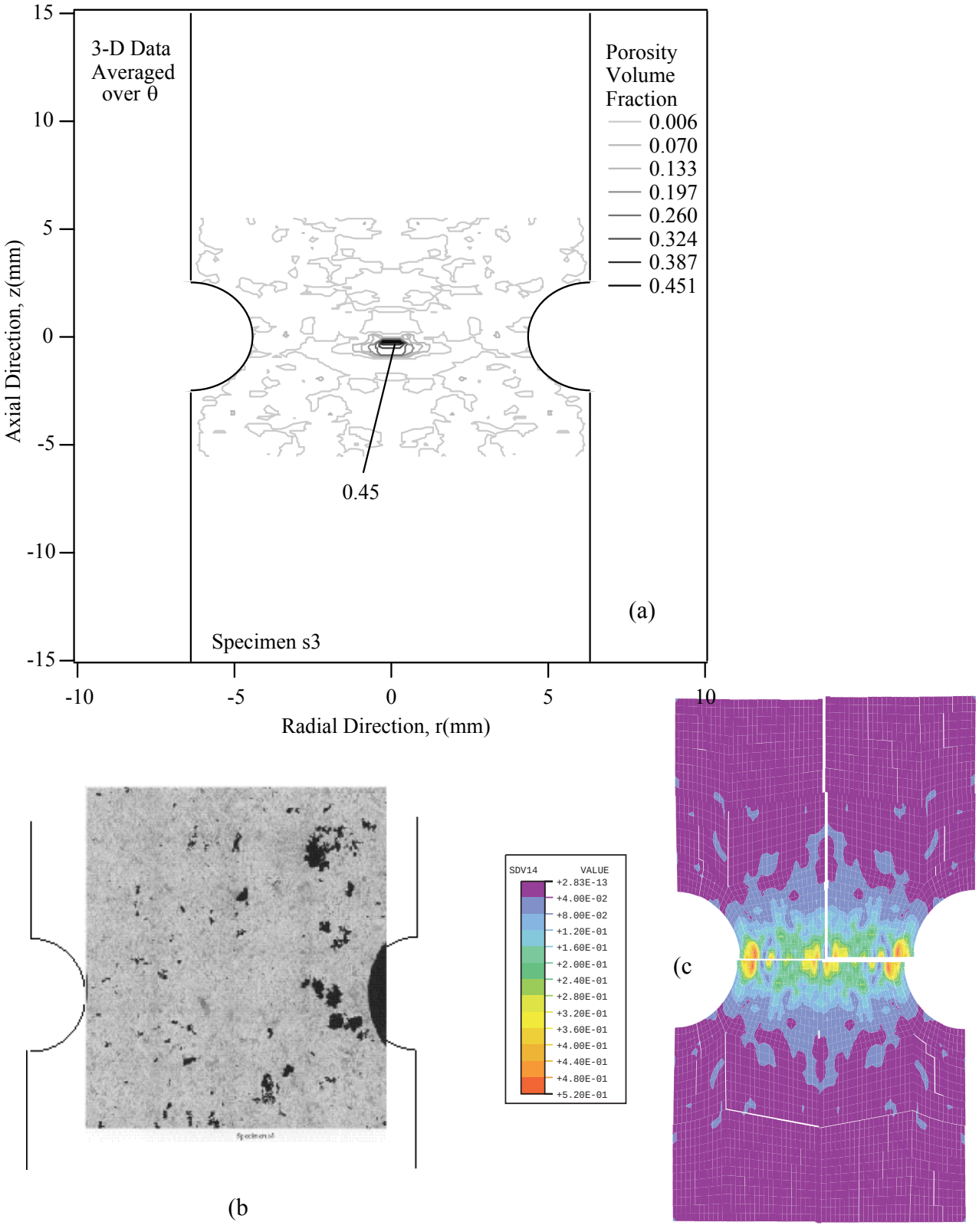

Figure 2. Pictorial illustration of porosity distribution for the 98% of failure load specimen from (a) x-ray tomography, (b) image analysis, and (c) finite element simulation with an initially random distribution of porosity at a level of 0.001.